JOURNAL OF CATALYSIS 139, 24–33 (1993)

Transport and Isomerization of Xylenes over HZSM-5 Zeolites

GABRIELE MIRTH, JIRÌ ČEJKA,[1] AND JOHANNES A. LERCHER[2]

Institut für Physikalische Chemie, Technische Universität Wien, Getreidemarkt 9, A-1060 Vienna, Austria

Received April 14, 1992; revised July 14, 1992

The diffusion, adsorption, and reaction of xylenes on HSZM-5 was investigated by means of time-resolved *in situ* FTIR spectroscopy and gas chromatography. The different diffusion coefficients determined for the three xylene isomers ($p:o:m \approx 1000:10:1$) were found to influence the isomerization rate above 523 K under the reaction conditions employed. Below that temperature, reactant diffusion played a minor role. For all xylene molecules, the intramolecular mechanism of isomerization suffices to account for all observations. The selectivity of *m*-xylene isomerization was found to depend primarily upon the transition entropy (transition state selectivity). The selectivity in *o*- and *p*-xylene depends upon the surface concentration of the primary product, *m*-xylene. Its concentration is a function of the activity of the catalyst and the diffusional constraints *m*-xylene faces. The decrease of the effectiveness of ZSM-5 above 523 K due to reactant diffusional constraints can be seen in lower coverages of *m*- and *o*-xylene in comparison to *p*-xylene.

INTRODUCTION

Over the last 20 years, the shape-selective formation of substituted aromatic molecules over medium-pore zeolites were intensely studied by industrial as well as academic institutions (e.g., *1–8*). Starting with the pioneering work of Chen *et al.* (*9*) the interest was mainly focused upon ZSM-5 as catalyst and was leading to several commercial processes (*10–13*). Thus, the kinetics of the alkylation, disproportionation, and isomerization reactions of aromatic molecules leading to xylenes and diethylbenzenes are well established (e.g., *2–4, 7, 8, 14*) and several models to explain the catalytic reactivities and selectivities have been advanced. The unique property of ZSM-5 [and in particular of chemically modified ZSM-5 (*1, 2, 5, 15, 16*)] is to produce *p*-dialkylbenzenes in selectivities exceeding the thermodynamic values by far. Because the kinetics of these reactions are, however, diffusion disguised, it is difficult to extract the reasons for this selectivity from the kinetic analysis of the overall process (*17*).

Based on these kinetic experiments, it was advanced that the transport limitation of the more bulky isomers (*m*-, *o*-) permits the faster diffusing products (*p*-) to escape from the catalyst at a higher rate and, thus, a higher selectivity toward the *p*-products was observed (*1, 4, 18*). In contrast, it was also suggested that the transition state leading to *p*-substituted products is more favorable than that for the other isomers (*1, 15, 19*). While there is increasing evidence that at least at higher temperatures diffusion plays a key role, the conclusions are not generally accepted. At this point it should be emphasized that the selectivity strictly depends upon the conversion (*20*) reaching equilibrium values when the conversion reaches equilibrium.

We have shown in a previous paper by using *in situ* IR spectroscopy (*8*) that the reaction in the pores may vary considerably with the reaction temperature and that it is difficult to extrapolate conclusions over a wide temperature range. The method has

[1] On leave from the J. Heyrovsky Institute for Physical Chemistry and Electrochemistry, Czechoslovak Academy of Sciences, Dolejskova 3, 182 23 Prague 8, Czechoslovakia.

[2] To whom correspondence should be addressed.

0021-9517/93 $5.00

the distinct advantage over standard catalytic techniques that the surface coverage and the reaction rate can be determined simultaneously and independently from each other. In this paper we report results on the xylene isomerization over HZSM-5 under steady-state and non-steady-state conditions.

EXPERIMENTAL

Material

For all investigations, a zeolite HZSM-5 with a Si/Al ratio of 35.5 (corresponding to 2.6 Al atoms per unit cell) was used. As determined by scanning electron microscopy, the size of the nearly spherical polycrystalline zeolite particles is approximately 1 μm. The sample was provided in the ammonium exchanged form and was converted to the protonic form by heating the zeolite in vacuum (pressure below 10^{-6} mbar) up to 923 K or in He flow (~20 ml/min) up to 773 K with a heating rate of 10 K/min.

FTIR Spectroscopy

The sample was analyzed *in situ* during all treatments by means of transmission absorption IR spectroscopy using a Bruker IFS 88 FTIR spectrometer (resolution 4 cm^{-1}). For the IR measurements the zeolite was pressed into self-supporting wafers and placed in a sample holder in the center of the furnace of the IR cell. The spectra were normalized for the sample thickness by comparing the intensities of the absorption bands of the adsorbate with the intensities of the lattice vibration bands of the zeolite between 2090 and 1740 cm^{-1}. Two different types of experiments were designed to show the adsorption/desorption and reaction behavior under static and flow conditions:

(i) For the first type of experiments (static conditions) a sample compartment, which could be evacuated to pressures below 10^{-6} mbar, was used (*21*). The xylene isomers were introduced into the vacuum system via a gas inlet manifold. The activated zeolite was contacted with 1 mbar of the adsorbate at constant temperature until adsorption–desorption equilibrium was achieved. During adsorption, IR spectra were collected with time resolutions between 10 s and 10 min, depending on the rates of adsorption of the substances. The coverage of the strong Brønsted acid sites (Si–OH–Al groups) with xylenes was determined from the decrease in the intensity of the OH stretching vibration at 3610 cm^{-1} upon interaction with the xylene molecules. The temperature of adsorption was varied from 373 to 573 K. From the time-dependent uptake, the diffusion coefficients were estimated.

(ii) For the second type of experiments (flow conditions) an IR cell, which approximates a continuously stirred tank reactor (volume = 1.5 cm^3), equipped with $\frac{1}{16}$-in. gas inlet and outlet tubing and CaF_2 windows, was used (*8*). The effluent gas stream was sampled in 16 sample loops of a multiport valve and subsequently analyzed by means of gas chromatography (HP 5890 II, capillary column DBWAX, 30 m). This experimental setup allows a simultaneous analysis of the product inside the zeolite pores (IR spectroscopy) and in the gas phase (GC). The experiments were carried out in continuous-flow mode in a temperature interval from 473 to 573 K. To achieve xylene conversions in the range 1–10% for all experiments, partial pressures of helium and xylene of 0.984 and 0.016 bar were used, respectively. For the characterization of the surface species in the zeolite pores during the reaction, IR spectra of the catalyst were recorded as the activated zeolite was contacted with a xylene containing He stream (with an initial time resolution of 30 s and of 5 min after 5 min time on stream). Simultaneously, samples of the effluent gas stream were collected in the 16 sample loops of the multiport valve with a time resolution of 30 s during the first 5 min and of 10 min afterward. After 1 h time on stream, the feed was switched to pure He for 15 min at the same temperature. Thus, all molecules with a mean residence time smaller than 15 min should desorb from the zeolite pores.

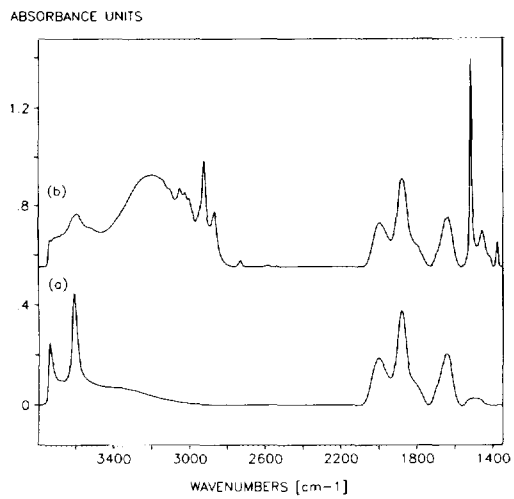

FIG. 1. IR spectra of (a) the activated zeolite HZSM-5 at 373 K and (b) *p*-xylene adsorbed at HZSM-5 at 373 K.

RESULTS

The IR spectrum of the activated zeolite HZSM-5 (see Fig. 1a) showed two bands of OH stretching vibrations at 3610 cm^{-1} (attributed to the Si–OH–Al groups, the strong Brønsted acid sites) (*22*, *23*) and 3745 cm^{-1} (attributed to silanol groups) (*24*).

(*i*) *Adsorption of Pure Xylene Isomers under Static Conditions*

The wavenumbers of the adsorption maxima of the characteristic IR bands (*25*, *26*) of the adsorbed xylene isomers at 373 K are compiled in Table 1. The band shifts due to temperature and coverage effects were in the range of ± 5 cm^{-1}.

p-Xylene. For all adsorption temperatures, adsorption–desorption equilibrium was achieved within a few seconds after contact of 1 mbar *p*-xylene with the zeolite. The OH band of the zeolite at 3610 cm^{-1} was broadened and shifted to lower wavenumbers due to hydrogen bonding between the Si–OH–Al group and the aromatic ring of the xylene molecule (see Fig. 1b). The shift was approximately 425 cm^{-1} (3610 → 3185 cm^{-1}), which indicates that hydrogen bonds of substantial strength exist between the Brønsted acid sites and the aromatic molecule (*27*, *28*). In contrast, the band of the OH stretching vibration of the Si–OH groups was shifted only by about 145 cm^{-1} (3745 → 3600 cm^{-1}) upon interaction with xylene, suggesting much weaker interaction. The coverage of the strong Brønsted acid sites and of the silanol groups was complete at 373 K and 1 mbar of *p*-xylene. At 473 and 573 K, approximately 60 and 12% of the Si–OH–Al groups were covered, respectively. Only small amounts of *p*-xylene were adsorbed on the silanol groups above 473 K. It should be noted that although the intensity of the band at 3610 cm^{-1} decreased by about 12% at 573 K after admission of 1 mbar of *p*-xylene, only CH- and ring vibration bands of low intensity were found in the IR spectra. This might be speculatively attributed to high mobility of the molecules

TABLE 1

Wavenumbers of the Characteristic IR Bands of the Adsorbed Xylene Isomers (at 373 K) at the Zeolite HZSM-5

T = 373 K p = 1 mbar HZSM-5	CH-Stretching vibrations (cm^{-1})	Ring vibrations (cm^{-1})	CH-Deformation vibrations (cm^{-1})
p-Xylene	3050, 3025, 3007 2927, 2872	<u>1518</u>	1379
m-Xylene	3053, 3032 2926, 2868	<u>1610</u> 1485	1381
o-Xylene	3072, 3031 2977, 2951, 2931 2877	1604 (weak) <u>1496, 1466</u>	1390

Note. The bands used for the identification of the isomers are underlined.

within the zeolite pores. At 373 and 473 K, adsorbed reaction products were not detected in the zeolite pores. The low coverage at 573 K did not permit an identification of adsorbed isomerization products.

o-Xylene. Adsorption–desorption equilibrium of 1 mbar *o*-xylene with the zeolite was achieved after about 4 h contact time at 373 K, after 40 min at 473 K and after a few minutes at 573 K. The coverage of the strong Brønsted acid sites was complete at 373 K, approximately 60% at 473 K and 10% at 573 K. The characteristic IR bands for *o*-xylene adsorbed on HZSM-5 (see Fig. 2) are compiled in Table 1. Bands that could be assigned to compounds other than *o*-xylene were not detected under the experimental conditions used.

m-Xylene. Equilibrium of 1 mbar *m*-xylene with HZSM-5 at 373 K was achieved after approximately 14 h, at 473 K after 3.5 h, and at 573 K after 5 min. The coverage of the strong Brønsted acid sites achieved after adsorption of 1 mbar of *m*-xylene at 373 K was 65–70%. At 473 K, ~60% of the Brønsted acid sites were covered. At 573 K, the decrease of the intensity of the Si–OH–Al groups upon interaction with *m*-xylene was approximately 12%. *m*-Xylene also adsorbed on the silanol groups at 373 K, but only a small fraction of the Si–OH groups interacted with the aromatic molecules at 473 and 573 K.

(ii) Diffusion of the Xylene Isomers

From the time-dependent uptake of the pure xylene isomers at constant temperature, the diffusion coefficients were estimated according to Refs. (*29*, *30*). The uptake (Q) was determined from the normalized intensities of the characteristic IR band of the adsorbate. Since the values of the effective non-steady-state diffusivities are highly temperature and concentration dependent (*31*), all measurements were carried out at 373 K at a xylene partial pressure of 1 mbar. Assuming that our catalyst consists of spherical particles ($r_0 = 0.5\ \mu$m), the following equation was used to estimate the diffusion coefficients for the xylene isomers:

$$Q_t/Q_\infty = 6/r_0 \cdot (Dt/\pi)^{0.5}.$$

In this equation, Q_t denotes the uptake at time (t) and Q_∞ the uptake after equilibration. The slope of the linear part of the curve (from $Q_t/Q_\infty = 0.3$ to 0.6) was used to estimate the diffusion coefficients (D). As an example, the normalized intensity of the ring vibrations of *o*-xylene at 1496 + 1466 cm^{-1} is plotted versus the square root of the

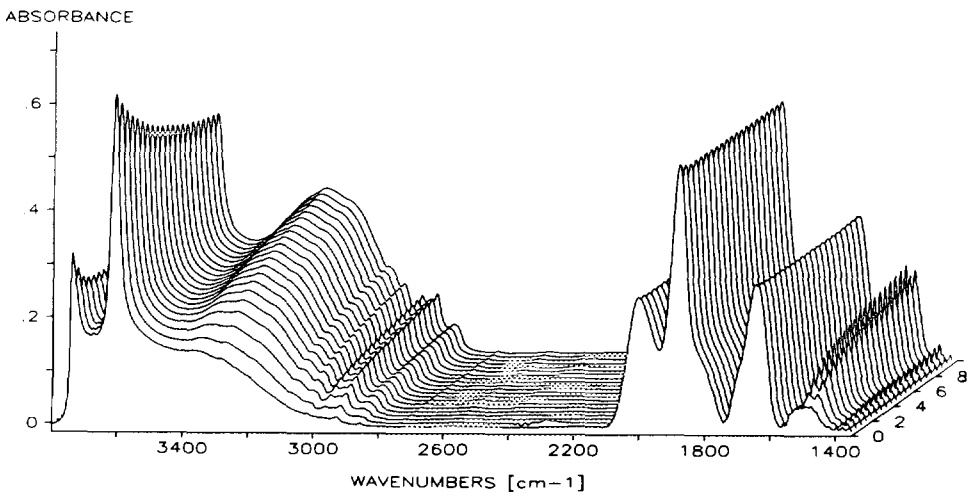

FIG. 2. Time-resolved IR spectra of the adsorption of *o*-xylene on HZSM-5 at 373 K (time resolution of 0.5 min, no equilibration).

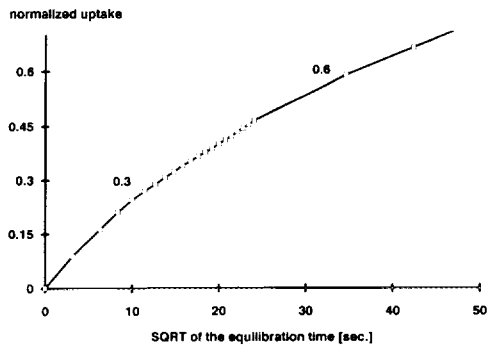

FIG. 3. Normalized intensity of a ring vibration of *o*-xylene plotted versus the square root of the equilibration time (T = 373 K).

equilibrium time (t) in Fig. 3. Because the diameter of the pore openings of the zeolite HZSM-5 (0.56 nm) is approximately of the size of a benzene ring (*32*, *33*), substituted aromatic molecules, e.g., xylenes, can face quite significant sterical hindrance within the confines of the zeolite pores. At 373 K and 1 mbar partial pressure, for *p*-xylene (the molecule with the smallest kinetic diameter), the diffusion coefficient was $D = 6.10^{-12}$ cm^2/s. This was two to three orders of magnitude higher than that for the bulkier isomers *o*-xylene ($D = 6 \times 10^{-14}$ cm^2/s) and *m*-xylene ($D = 7 \times 10^{-15}$ cm^2/s) (*1*, *3*, *16*, *34*). The values of the diffusion coefficients at 373 and 473 K are given in Table 2. The energies of activation for the diffusion of *m*- and *o*-xylene were determined to be approximately 30 kJ/mol (*35*).

(iii) Xylene Reactions under Flow Conditions

The reaction of the pure xylene isomers was studied in a continuously stirred tank reactor. The reaction rates for the xylene isomerization were normalized for the concentration of the strong Brønsted acid sites (= turnover frequency, TOF, [molecules/site · s]). The values (±10%) of the TOFs after 1 h on stream determined at reaction temperatures between 473 and 573 K are summarized in Table 3.

Reaction at 473 K. At 473 K, after 1 h time on stream, approximately 70% of the Brønsted acid sites were covered when *p*- and *o*-xylene were isomerized, while 55% of these sites were occupied in the case of *m*-xylene isomerization. The analysis of the time-resolved IR spectra showed that adsorption/desorption equilibrium was reached after 1 min with *p*-xylene and after a few minutes of *o*-xylene. With *m*-xylene, approximately 50% of the acid sites were covered within the first 10 min. With increasing reaction time, the coverage increased slightly to reach 55% after 1 h (see Fig. 4).

Analysis of the IR spectra of the adsorbed phase revealed that in all cases the reacting isomer was the main adsorbate. However, a buildup of *m*-xylene in the zeolite pores (indicated by the appearance of the characteristic bands at 1610 and 1485 cm^{-1}) with increasing time on stream was found for *o*- and *p*-xylene isomerization (see Fig. 5). After 1 h time on stream, approximately 8% (in the case of *p*-xylene reaction) and 15% (in the *o*-xylene isomerization) of the acid sites were covered with *m*-xylene molecules. When *m*-xylene was the reactant, the

TABLE 2

Values of the Diffusion Coefficients at 373 and 473 K (p_t = 1 mbar)

	D (cm^2/s) at 373 K	D (cm^2/s) at 473 K	ΔE_a (kJ/mol)
p-Xylene	6×10^{-12}	—	—
o-Xylene	6.5×10^{-14}	5×10^{-13}	30
m-Xylene	7×10^{-15}	5×10^{-14}	29

TABLE 3

Reaction Rates Normalized per Acid Site for the Xylene Isomerization over HZSM-5 between 473 and 573 K after 1 h Time on Stream (TOF ±10%)

TOF (±10%) (molecules/site · s)	T = 473 K	T = 523 K	T = 573 K
p-Xylene	0.0012	0.0044	0.0088
m-Xylene	0.0013	0.0037	0.0054
o-Xylene	0.0011	0.0044	0.0067

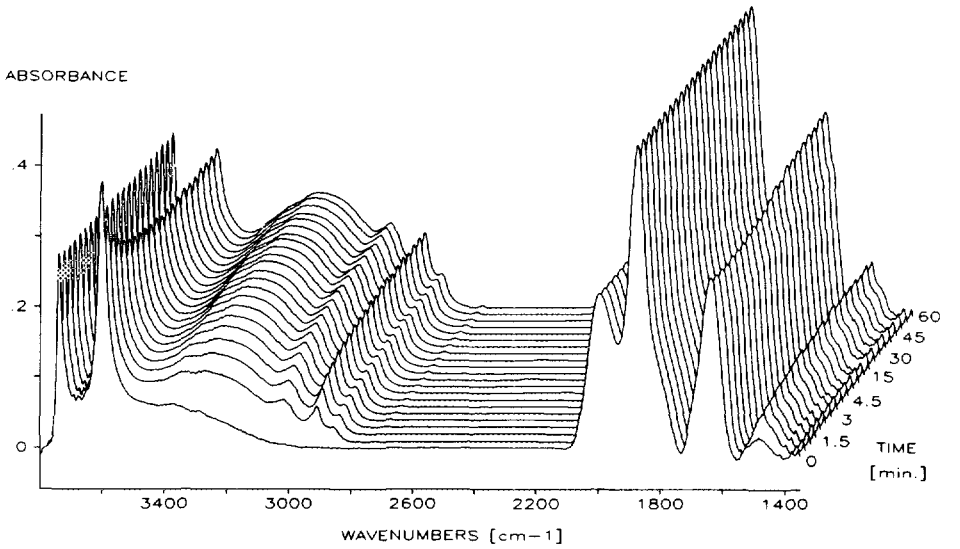

FIG. 4. Time-resolved IR spectra of the adsorption/reaction of *m*-xylene with HZSM-5 at 473 K under flow conditions.

intensities of the bands of isomerization products were below the detection limit. This indicates that comparable surface concentrations of the reactant were observed for all three isomers after 1 h time on stream.

The analysis of the effluent gas stream showed that the turnover frequency, defined as the reaction rate per acid site of the catalyst, gave similar values for all three isomers, i.e., $\sim 1.2 \times 10^{-3}$ molecules/site · s. For *m*-xylene, the increase in the reaction rate (TOF) was found to be directly proportional to the increase in coverage as determined from the IR spectra (see Fig. 6). With

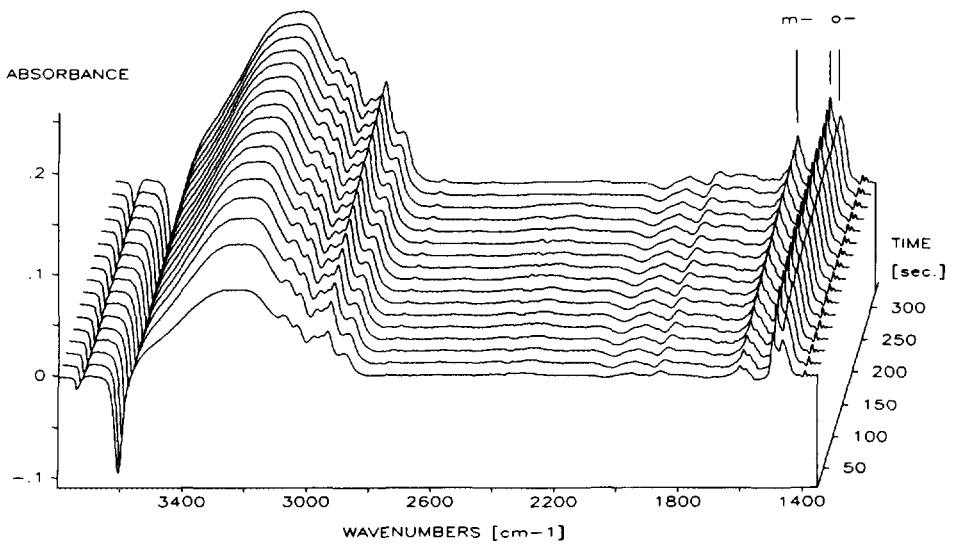

FIG. 5. Time-resolved difference IR spectra of the adsorption/reaction of *o*-xylene with HZSM-5 at 473 K under flow conditions (time resolution 20 s).

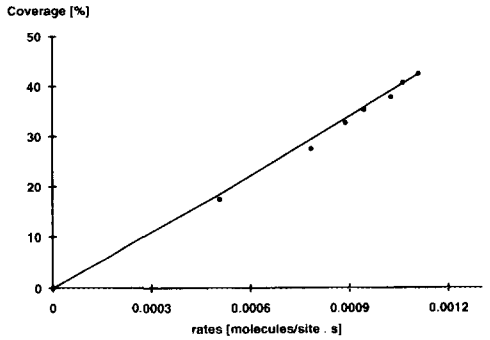

FIG. 6. Reaction rate of the *m*-xylene isomerization at 473 K (determined from the gas analysis) plotted versus the coverage as determined from the IR spectra.

p-xylene as reactant, this correlation was not observed. While the coverage raised up to nearly 60% immediately after admitting *p*-xylene into the reactor, a slower increase in the concentration of the products in the gas phase was observed within the first minutes on stream. The transient behavior for *o*-xylene isomerization was found to be similar to that noted for *p*-xylene in the first minute of reaction. Additionally, an increasing reaction rate with increasing coverage was found for the following minutes.

The ratio of the isomerization products in the gas phase after 1 h time on stream was found to be $p/o \approx 2$ for the isomerization of *m*-xylene, $m/o \approx 5$ for the reaction of *p*-xylene, and $m/p \approx 3.5$ for the reaction of *o*-xylene. It should be especially emphasized that for the isomerization of *m*-xylene, the concentration of *p*-xylene in the gas phase was twice as high as that of *o*-xylene. Disproportionation products, i.e., toluene and trimethylbenzene isomers, were not detected in the gas phase or in the adsorbed phase.

After reaction, IR spectra were monitored during purging the catalyst with pure He at reaction temperature for 15 min. After *o*- and *p*-xylene isomerization, the unreacted molecules desorbed within a few minutes and the *m*-xylene molecules produced during the reaction desorbed at a much lower rate. In the case of *m*-xylene isomerization, nearly all adsorbed *m*-xylene molecules desorbed during the 15 min of purging; only low concentrations of an unknown hydrocarbon species with IR bands at 2925, 1685, 1633, 1585, and 1450 cm^{-1} (formed during the reaction in the zeolite) remained at the surface.

Reaction at 523 K. From the changes in the IR spectra recorded during reaction at 523 K it was concluded that after 1 h time on stream, about 15% of the acid sites were covered during *m*-xylene isomerization and approximately 25% during *o*- and *p*-xylene isomerization. Adsorption–desorption equilibrium was achieved within the first minutes of contact for all three isomers. The analysis of the adsorbed phase indicated that during the *o*- and *p*-xylene isomerization (in addition to the adsorbed reactant molecules) about 33 and 25% of the adsorbed molecules were *m*-xylene, respectively. It should be noted, however, that the coverages were determined with an accuracy of ±10 rel.% only.

From the gas-phase concentrations of the products, the TOF for the isomerization reaction was calculated to be 4.4×10^{-3} molecules/site · s for *o*- and *p*- xylene and slightly lower for *m*-xylene. The changes of the reaction rates of the different isomers with increasing temperature are shown in Fig. 7. For *m*-xylene, the product composition determined after 1 h time on stream ($p/o \approx 2$) did not change compared to the situation at 473 K. For the *o*-xylene and *p*-xylene

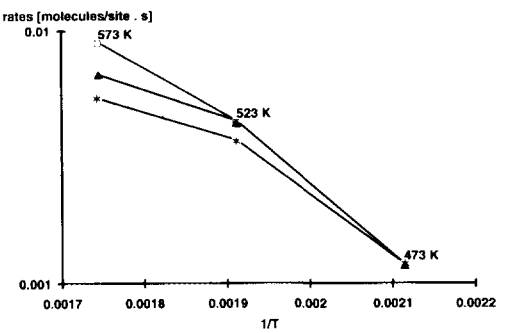

FIG. 7. Changes of the reaction rates of the xylene isomers with increasing temperature. (□) *p*-xylene, (*) *m*-xylene, (▲) *o*-xylene.

isomerization, the *m/p* and *m/o* xylene ratio shifted to lower values (*o*, 3.5 → 1.8; *p*, 5 → 3.8).

IR bands assigned to adsorbed xylene molecules were not observed after purging the catalyst for a few minutes. The remaining adsorbed species blocked about 3–5% of the strong Brønsted acid sites and had absorption bands at 2925 and 1585 cm^{-1}.

Reaction at 573 K. At 573 K, the IR spectra showed only low intensities of the bands attributed to adsorbed surface species. After 1 h time on stream, approximately 3–5% of the acid sites were covered when *m*-xylene was used as reactant. In the case of *o*- and *p*-xylene isomerization, a xylene coverage of about 11 and 13% with xylene molecules was achieved, and about 45 and 35% of these were found to be *m*-xylene, respectively. The difference to 100% was the reactant isomer. With increasing time on stream a buildup of low concentrations of unidentified hydrocarbon species was noted. The isomerization rates were different for the three xylene isomers. For *p*-xylene the highest TOF (8.8×10^{-3} molecules/site · s) was determined, for *o*-xylene it was about 6.7, and for *m*-xylene it was 5.4×10^{-3} molecules/site · s.

DISCUSSION

The adsorption kinetics of the single xylene isomers on HZSM-5 under nonreactive conditions (373 K) confirm previous conclusions (e.g., *1, 2, 36*) that the pore structure of medium-pore zeolites imposes sterical restrictions on the transport of *m*- and *o*-substituted aromatic molecules relative to the *para*-isomers. The estimation of the diffusion coefficients from IR measurements of the pure xylene isomers indicated a ratio of the diffusion coefficients for *p* : *o* : *m*-xylene of 1000 : 10 : 1. The difference in the diffusion coefficients of *p*- and *m*-xylene by a factor of 1000 is in excellent agreement with the assumption of Wei (*34*). However, Wei (*34*) and Chen (*4*) assumed equal values for *o*- and *m*-xylene. This differs from the 10 times higher diffusion coefficient we found for *o*-xylene than for *m*-xylene. A similar result was reported by Choudhary and Akolekar (*37*).

Although big differences in the rate of adsorption were found for the three isomers, the equilibrium surface coverage found for *p*-, *m*,-, and *o*-xylene was identical at elevated temperatures. This indicates identical adsorption constants for all three isomers. At low adsorption temperatures (373 K), in contrast to the complete coverage achieved with *p*- and *o*-xylene, only 65–70% of the Brønsted acid sites were covered with *m*-xylene molecules. Because we concluded from the measurements at 473 and 573 K that all three xylene isomers have identical adsorption constants, the lower coverage of *m*-xylene at 373 K can only be explained by steric hindrance of the adsorption at a part of the Brønsted acid sites. Note that the identical adsorption constants were also confirmed by adsorption experiments of equilibrium mixtures of the xylenes at 373 K (*7*). A partial exclusion of *m*-xylene from the pores of ZSM – 5 at low temperatures (423 K) has already been reported by Chen (*4*), but no explanation for this phenomenon was given.

The rate of isomerization of *m*-xylene was found to increase in parallel with the coverage under steady state and transient conditions. Consequently, it was concluded that all sites that adsorb *m*-xylene catalyze the isomerization with the same rate. When *o*- or *p*-xylene were used as reactants, differences in the transient behavior of the isomerization reaction were observed. After the stepwise pressure increase, a high initial reactant uptake and an accumulation of *m*-xylene in the pores was detected, but low turnover frequencies were determined within the first minutes of time on stream. These low initial TOF values are concluded to be caused by the accumulation of *m*-xylene in the zeolite pores. Thus, only a part of the products formed was released into the gas phase. It should be emphasized that during the transient stage, this accumulation

leads to an increase in the rate of diffusion of *m*-xylene and of the secondary isomerization to *o*-xylene and *p*-xylene.

Under steady-state conditions, all reacting xylenes had the same surface concentration and the same reaction rate at 473 K. Thus, we concluded that the rate constant was identical for all three isomers. It also shows that the surface reaction and not the diffusion of the reactants is the rate-determining step of the overall reaction. The reactant isomer was the main species adsorbed on the catalyst. For *p*- and *o*- xylene, additional accumulation of *m*-xylene molecules in the pores was observed. The relative concentration of adsorbed *m*-xylene directly determines the extent of the secondary reaction. These results are consistent with the proposal (*2, 3*) of a unimolecular mechanism of the xylene isomerization over HZSM-5. For zeolites with a low Si/Al ratio and narrow channels, Corma and Sastre (*38*) proposed that xylene isomerization proceeds via the unimolecular 1.2. methyl shift.

At 573 K, the reaction rate for the isomerization decreased in the sequence *p*-xylene > *o*-xylene > *m*-xylene, demonstrating that the diffusivity of the reactant molecules influences the overall reaction rate. The differences in the diffusivity are also reflected in the different reactant coverages which are directly proportional to the catalyst efficiency (*20*) (coverages $p \approx 8.5\%$, $o \approx 6\%$, $m \approx 3\%$). With *p*- and *o*-xylene as reactants, approximately 35 and 45% of the molecules adsorbed at steady state were *m*-xylene. Again, the relative surface concentration of *m*-xylene reflects qualitatively the amount of secondary reactions. The *m/o* ratio was approximately 3 (reacting *p*-xylene), while the *m/p* ratio was approximately 1.7 (reacting *o*-xylene). Note that the relative coverage of *m*-xylene and the extent of the secondary reaction increase with the reaction temperature. We emphasize that these results are in perfect agreement with the model assuming the isomerization of the xylenes in medium pore zeolites to proceed via an intramolecular 1,2 methyl shift (*2, 3, 17*).

For *m*-xylene isomerization, the ratio *p/o* was 2 for all temperatures investigated. This suggests that both reactions (i.e., the *m*-xylene isomerization to *p*- and to *o*-xylene) have the same apparent energies of activation. Thus, the differences in the preexponential factor in the Arrhenius equation must account for the selectivities observed and are tentatively attributed to differences in the transition entropy. One would expect that the transition state to form *o*-xylene is more bulky than that to form *p*-xylene. Molecular modeling indeed shows that the minimum kinetic diameters of the transition state complexes in the *meta* → *para* and *meta* → *ortho* xylene isomerization are 0.62 nm and 0.67 nm, respectively. Thus, the constraints for the formation of the transition state should be larger for the *meta* → *ortho*-intermediate than for the *meta* → *para*-intermediate. Hence, the transition entropy (and therefore the preexponential factor) should be lower for the *meta* → *ortho*-transition state. This suggests that the *p/o* ratio of 2 in the *m*-xylene isomerization can be explained by restricted transition state selectivity. Note that (in the absence of these constraints) *m*-xylene isomerization over amorphous silica–alumina catalysts exhibited *p/o* ratios of 1.2 (*39*).

CONCLUSIONS

Investigations of the adsorption kinetics of the pure xylene isomers under nonreactive conditions resulted in differences in the diffusion coefficients of the isomers of $p:o:m = 1000:10:1$. Despite the big differences in the rates of transport, comparable adsorption constants were found for all three isomers.

In the isomerization reactions of the pure xylene isomers over HZSM-5, equal rates of reaction were detected for all three xylenes at low temperature. These identical values of the reaction rates suggest the absence of reactant diffusion limitation at 473 K. The reaction rates were found to be direct proportional to the surface concentrations of the reactant isomers. Thus, all three

xylene isomers are converted with the same reaction constant. With increasing reaction temperature, a transition from a surface reaction-controlled regime to a reactant diffusion-controlled regime was noted. The surface concentration of the reactant isomer and in parallel the reaction rate increased with increasing diffusivity of the reactant, i.e., in the order *p*-xylene > *o*-xylene > *m*-xylene. The results are in perfect agreement with the model of the unimolecular reaction mechanism in xylene isomerization. Secondary isomerization reactions gained in importance when the *m*-xylene coverage (for isomerization of *p*- and *o*-xylene) and the reaction temperature increased. A product ratio *p*/*o* of 2 in the case of *m*-xylene reaction was observed for all temperatures investigated and concluded to be caused by restricted transition state selectivity.

ACKNOWLEDGMENTS

This work was supported by the "Christian Doppler Laboratory for Heterogeneous Catalysis" and by the "Fonds zur Förderung der Wissenschaftlichen Forschung" under Project P7312. We are grateful to Ernst Nusterer for carrying out theoretical estimations of the dimensions of the transition states by molecular modelling.

REFERENCES

1. Kaeding, W. W., Chu, C., Young, L. B., Weistein, B., and Butter, S. A., *J. Catal.* **67,** 159 (1981).
2. Young, L. B., Butter, S. A., and Kaeding, W. W., *J. Catal.* **76,** 418 (1982).
3. Olson, D. H., and Haag, W. O., *Am. Chem. Soc. Symp. Ser.* **248,** 275 (1984).
4. Chen, N. Y., *J. Catal.* **114,** 17 (1988).
5. Kürschner, U., Jerschkewitz, H. G., Schreier, E., and Völter, J., *Appl. Catal.* **57,** 167 (1990).
6. Chen, N. Y., Garwood, W. E., and Dwyer, F. G., *in* "Shape Selective Catalysis in industrial Applications." Dekker, New York, 1989.
7. Vinek, H., and Lercher, J. A., *J. Mol. Catal.* **64,** 23 (1991).
8. Mirth, G., and Lercher, J. A., *J. Catal.* **132,** 244 (1991).
9. Chen, N. Y., Kaeding, W. W., and Dwyer, F. G., *J. Am. Chem. Soc.* **101,** 6783 (1979).
10. Haag, W. O., and Olson, D. H., *U. S. Patent* 3,856,871 (1974).
11. Kaeding, W. W., and Butter, S. A., *U.S. Patent* 3,911,041 (1975).
12. Butter, S. A., and Young, L. B., *U.S. Patent* 3,965,209 (1976).
13. Kaeding, W. W., and Young, L. B., *U.S. Patent* 4,034,053 (1977).
14. Cejka, J., Wichterlova, B., and Bednarova, S., *Appl. Catal.* **79,** 215 (1991).
15. Sayed, M. B., and Vedrine, J. C., *J. Catal.* **101,** 43 (1986).
16. Sayed, M. B., Auroux, A., and Vedrine, J. C., *J. Catal.* **116,** 1 (1989).
17. Bauer, F., Dermietzel, J., and Jockisch, W., *Stud. Surf. Sci. Catal.* **65,** 305 (1991).
18. Nunan, J., Cronin, J., and Cunningham, J., *J. Catal.* **87,** 77 (1984).
19. Bezouhanova, C., Dimitrov, C., Nrova, V., Spassov, B., and Lerchert, H., *Appl. Catal.* **21,** 149 (1986).
20. Richter, M., Fiebig, W., Jerschewitz, H.-G., Lischke, G., and Öhlmann, G., *Zeolites* **9,** 238 (1989).
21. Jentys, A., Warecka, G., and Lercher J. A., *J. Mol. Catal.* **51,** 309 (1989).
22. Jacobs, P. A., and van Ballmoos, R. J., *J. Phys. Chem.* **86,** 3050 (1982).
23. Hatada, K., Ono, Y., and Ushiki, Y., *Z. Phys. Chem.* **117,** 37 (1979).
24. Gallei, E., and Eisenbach, D., *J. Catal.* **37,** 474 (1975).
25. Bellamy, L. J., "The Infrared Spectra of complex molecules," pp. 73–96. Chapman & Hall, London, 1975.
26. Colthup, N. B., Daly, L. H., and Wiberly, S. E., "Introduction to Infrared and Raman Spectroscopy," pp. 257–269. Academic Press, New York, 1975.
27. Hair, M. L., and Hertl, W., *J. Phys. Chem.* **74,** 91 (1970).
28. Mirth, G., and Lercher, J. A., *J. Phys. Chem.* **95,** 3736 (1990).
29. Breck, D. W., "Zeolite Molecular Sieves," pp. 671–670. Wiley, New York, 1974.
30. Choudhary, V. R., and Singh, A. P., *Zeolites* **6,** 206 (1986).
31. Garcia, S. F., and Weisz, P. B., *J. Catal.* **121,** 294 (1990).
32. Hashimoto, K., Masuda, T., and Kawase, M., *Stud. Surf. Sci. Catal.* **46,** 485 (1989).
33. Csicsery, S. M., *Zeolites* **4,** 202 (1984).
34. Wei, J., *J. Catal.* **76,** 433 (1982).
35. Ruthven, D. M., Eic, M., and Richard, E., *Zeolites* **11,** 747, 1991.
36. Kürschner, U., Jerschkewitz, H.-G., Schreier, E., and Völter, J., *Appl. Catal.* **57,** 167 (1990).
37. Choudhary, V. R., and Akolekar, D. B., *J. Mol. Catal.* **60,** 173 (1990).
38. Corma, A., and Sastre, E., *J. Chem. Soc. Chem. Commun.*, 594 (1991).
39. Dewing, J., *J. Mol. Catal.* **27,** 25 (1984).